

## Muon spin relaxation study of spin dynamics in the extended kagome systems $\text{YBaCo}_4\text{O}_{7+\delta}$ ( $\delta = 0, 0.1$ )

S. Lee,<sup>1</sup> Wonjun Lee,<sup>1</sup> K. J. Lee,<sup>2</sup> ByungJun Kim,<sup>2</sup> B. J. Suh,<sup>2</sup> H. Zheng,<sup>3</sup> J. F. Mitchell,<sup>3</sup> and K.-Y. Choi<sup>1,\*</sup>

<sup>1</sup>*Department of Physics, Chung-Ang University, 84 Heukseok-ro, Seoul 06974, Republic of Korea*

<sup>2</sup>*Department of Physics, The Catholic University of Korea, 43 Jibong-ro, Bucheon 14662, Republic of Korea*

<sup>3</sup>*Materials Science Division, Argonne National Laboratory, Argonne, Illinois 60439, USA*



(Received 30 May 2017; revised manuscript received 27 February 2018; published 15 March 2018)

We present muon spin relaxation ( $\mu\text{SR}$ ) measurements of the extended kagome systems  $\text{YBaCo}_4\text{O}_{7+\delta}$  ( $\delta = 0, 0.1$ ), comprising two interpenetrating kagome sublattices of  $\text{Co(I)}^{3+}$  ( $S = 3/2$ ) and a triangle sublattice of  $\text{Co(II)}^{2+}$  ( $S = 2$ ). The zero- and longitudinal-field  $\mu\text{SR}$  spectra of the stoichiometric compound  $\text{YBaCo}_4\text{O}_7$  unveil that the triangular subsystem orders at  $T_N = 101$  K. In contrast, the muon spin relaxation rate pertaining to the kagome subsystem shows persistent spin dynamics down to  $T = 20$  K and then a sublinear decrease  $\lambda(T) \sim T^{0.66(5)}$  on cooling towards  $T = 4$  K. In addition, the introduction of interstitial oxygen ( $\delta = 0.1$ ) is found to drastically affect the magnetism. For the fast-cooling experiment ( $>10$  K/min),  $\text{YBaCo}_4\text{O}_{7.1}$  enters a regime characterized by persistent spin dynamics below 90 K. For the slow-cooling experiment (1 K/min), evidence is obtained for the phase separation into interstitial oxygen-poor and oxygen-rich regions with distinct correlation times. The observed temperature, cooling rate, and oxygen content dependencies of spin dynamics are discussed in terms of a broad range of spin-spin correlation times, relying on a different degree of frustration between the kagome and triangle sublattices as well as of oxygen migration.

DOI: [10.1103/PhysRevB.97.104409](https://doi.org/10.1103/PhysRevB.97.104409)

### I. INTRODUCTION

Geometrically frustrated magnets provide a fascinating setting for observing exotic states of matter and their associated fractionalized quasiparticles [1]. The local connectivity of edge- and corner-sharing triangles offers an elementary motif of the geometrical frustrated magnets, in which antiferromagnetically coupled spins on triangular arrangements cannot simultaneously minimize their interaction energy [2,3]. This macroscopic degeneracy of a ground state aggrandizes quantum fluctuations among possible classical spin configurations, thereby preventing the formation of long-range magnetic order and destabilizing conventional magnon excitations in an extreme case.

A prototypical example of the frustrated magnets in two dimensions is triangular and kagome Heisenberg antiferromagnets, which are distinguished by a degree of frustration (=macroscopic degeneracy) and thus host a largely distinct ground state. The triangular Heisenberg model is widely accepted to have a  $120^\circ$  Néel ground state, yet it is highly susceptible to small perturbations, often stabilizing a quantum disordered state [4–11]. In contrast, the  $S = 1/2$  kagome Heisenberg antiferromagnets harbor gapped or gapless spin-liquid ground states [12–18]. These novel phases feature fractionalized spinon (charge neutral  $S = 1/2$ ) excitations and a lack of symmetry breaking down to  $T = 0$  K as exemplified in the herbertsmithite  $\text{ZnCu}_3(\text{OH})_6\text{Cl}_2$ , the best realization of the kagome lattice so far reported [19]. Given the dissimilar magnetism between the triangular and kagome lattices, it is

natural to ask about whether the two frustrated sublattices develop disparate spin correlations when they are combined into a single system.

The extended kagome compounds  $R\text{BaCo}_4\text{O}_7$  ( $R = \text{Y}$ , lanthanide) are a promising class of materials to address this issue. This is owed to the fact that  $R\text{BaCo}_4\text{O}_7$  consists of high-spin states of  $\text{Co(I)}^{3+}$  ( $S = 3/2$ ) and  $\text{Co(II)}^{2+}$  ( $S = 2$ ) ions arranged on a kagome and triangular lattice, respectively, which are stacked along the  $c$  axis in an alternating way [see Fig. 1(a)] [20,21]. Generically, depending on the ratio of  $J_2/J_1$  where  $J_1$  and  $J_2$  are the exchange interaction within the kagome layer and between the kagome and triangular layers, respectively, the ground state of  $R\text{BaCo}_4\text{O}_7$  ranges from spin liquid to nematic order, and to long-range order [22,23].

$\text{YBaCo}_4\text{O}_7$  crystallizes in a trigonal structure (space group  $P31c$ ) [24–27]. With decreasing temperature a structural phase transition occurs first at 310 K from the trigonal to an orthorhombic phase  $Pbn2_1$  and then to a monoclinic structure  $P2_1$  at 106 K. Noticeably, neutron diffraction experiments revealed that the low-temperature structural transition accompanies long-range antiferromagnetic ordering at  $T_N \sim 106$  K, followed by a subsequent spin reorientation around 60 K [26,27]. The concurrent magnetostructural ordering at 106 K implies strong spin-lattice coupling, which relieves partially the geometrical frustration [26,27]. From the Curie-Weiss fit to the magnetic susceptibility, a Curie-Weiss temperature is evaluated to  $\Theta_{\text{CW}} = -508$  K, yielding a moderate frustration parameter  $\Theta_{\text{CW}}/T_N \sim 5$  [27]. Remarkably, a  $^{59}\text{Co}$  NMR study unveils the different evolution of spin dynamics between the triangular and kagome subsystems. For temperatures of  $T < 4$  K, the triangular spins are antiferromagnetically ordered and the kagome spins are aligned orthogonal to the

\*kchoi@cau.ac.kr

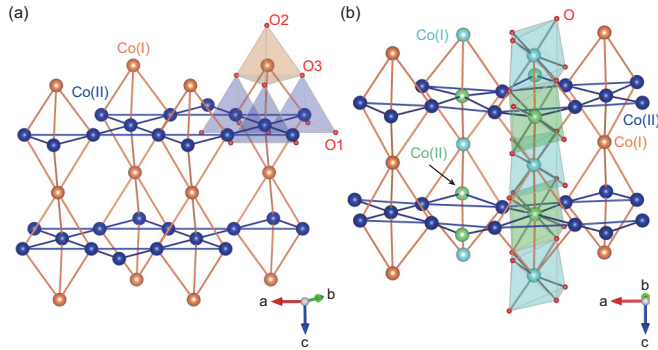


FIG. 1. (a) Sketch of the spin topology in the stoichiometric material  $\text{YBaCo}_4\text{O}_7$ . Orange and blue spheres represent two inequivalent Co atoms arranged on the triangular (solid orange lines) and kagome layers (solid blue lines). There are three crystallographically different oxygen sites (red small spheres) in the lattice. (b) Crystal structure of the oxygen-excess material  $\text{YBaCo}_4\text{O}_8$ . The cyan and light green spheres indicate the edge-sharing octahedral Co sites in the triangular and kagome planes, respectively. Introducing interstitial oxygen atoms leads to a conversion of the oxygen tetrahedra into octahedra.

triangular spins in a spin-flop configuration whose orientation contradicts the neutron diffraction results [28,29]. Unlike the triangular spins, the kagome spins become dynamically disordered with increasing temperature to 15 K and then form a two-dimensional viscous spin liquid for temperatures above 15 K [29].

The layered structure of  $\text{YBaCo}_4\text{O}_7$  facilitates the uptake of interstitial oxygens, producing the nonstoichiometric compound  $\text{YBaCo}_4\text{O}_{7+\delta}$  ( $0 < \delta < 1.6$ ) [30–33]. As sketched in Fig. 1(b), the interstitial oxygen atoms convert a fraction of the oxygen tetrahedra into octahedra surrounding Co ions, while changing the oxidation state of  $\text{Co}^{2+}$  to  $\text{Co}^{3+}$  [34,35]. It turned out that introducing a small amount of the excess oxygens to  $\text{YBaCo}_4\text{O}_7$  exerts a substantial impact on the structural and magnetic properties. In sharp contrast to  $\text{YBaCo}_4\text{O}_7$ ,  $\text{YBaCo}_4\text{O}_{7.1}$  retains the trigonal symmetry  $P31c$  down to 6 K without inducing long-range magnetic ordering [28,36]. It is remarkable that the magnetostructural transition is suppressed by the addition of extra oxygens. This suggests that structural disorders lead to a drastic weakening of magnetoelastic coupling and thus prohibit a lifting of macroscopic degeneracy.

The ac magnetic susceptibility of  $\text{YBaCo}_4\text{O}_{7.1}$  exhibits the frequency independent peak at 81 K, indicative of an unconventional spin glass phase [35]. The  $^{59}\text{Co}$  zero-field NMR measurements suggest that the triangular spins freeze-out while the kagome spins remain dynamically disordered at lower temperatures. In addition, in slow-cooling experiments the interstitial oxygens are separated into oxygen-rich and oxygen-poor regions [see Fig. 1(b) for the creation of the oxygen-rich region], forming a local inhomogeneous magnetic state. Taken together,  $\text{YBaCo}_4\text{O}_{7+\delta}$  is endowed with the panoply of dynamic and static as well as of homogeneous and inhomogeneous magnetism, relying on the cooling rate, sublattice exchange topology, and oxygen nonstoichiometry. As such, a spatiotemporal structure of spin correlations is

expected to vary with a time (frequency) window adopted for measurements. To gain further insight on the two distinct magnetic behaviors pertaining to the two spin subsystems, it is highly desirable to employ the muon spin relaxation ( $\mu\text{SR}$ ) technique whose time window bridges the gap between magnetic fluctuation rates probed with the NMR and neutron scattering techniques.

In this paper we report the zero-field (ZF)- and longitudinal-field (LF)- $\mu\text{SR}$  results of  $\text{YBaCo}_4\text{O}_{7+\delta}$  ( $\delta = 0, 0.1$ ) as a function of temperature, external field, and cooling rate. For the stoichiometric material, we observe sequential ordering processes occurring at  $T_N = 101$  K first in the triangle sublattice and then in the kagome sublattice upon cooling towards  $T = 4$  K. In contrast, the nonstoichiometric compound shows a weak magnetic order below 90 K while a large fraction of the spins remain in a fluctuating state at low temperatures. Depending on the cooling rate, the interstitial oxygen clustering gives rise to two heterogeneous magnetic entities.

## II. EXPERIMENTAL DETAILS

Single crystals of  $\text{YBaCo}_4\text{O}_{7+\delta}$  ( $\delta = 0, 0.1$ ) were grown by the optical floating-zone method [26]. Oxygen content was determined by quantitative thermogravimetric analysis of the ground crystal samples as described in Ref. [36].  $\mu\text{SR}$  experiments were carried out on the D1 spectrometer at J-PARC (Tokai, Japan) and with the LAMPF spectrometer at TRIUMF (Vancouver, Canada). The crystals were grounded and wrapped with a silver foil and attached to the sample holder. The mounted samples were then inserted into a cryostat with a temperature range  $T = 1.6\text{--}300$  K. At J-PARC, pulsed muon beams with a full width at half-maximum (FWHM) of 100 ns were implanted into the sample, while continuous muon sources in TRIUMF have no dominating time structure. The measured physical quantity is the evolution of the muon polarization  $P_z(t)$  given by

$$P_z(t) = \frac{N_B(t) - \alpha N_F(t)}{N_B(t) + \alpha N_F(t)}, \quad (1)$$

where  $N_F(t)$  and  $N_B(t)$  are the positron counts in the forward and backward detectors, which are parallel and antiparallel to an incident muon spin direction, respectively.  $\alpha$  is the efficiency ratio between the forward and backward detectors. The  $\alpha$  parameter was determined from a weak transverse field spectrum with  $H \sim 50$  Oe in a high-temperature paramagnetic state. In order to elucidate the spin dynamics of  $\text{YBaCo}_4\text{O}_{7+\delta}$ , we analyzed all of the  $\mu\text{SR}$  data measured in a zero field and a longitudinal field by using the free software package MUSRFIT.

## III. RESULTS AND DISCUSSION

### A. $\text{YBaCo}_4\text{O}_7$

To differentiate spin dynamics between the triangular and kagome sublattices, we performed both ZF- and LF- $\mu\text{SR}$  measurements with the LAMPF spectrometer at TRIUMF. Figure 2(a) presents the ZF- $\mu\text{SR}$  spectra of  $\text{YBaCo}_4\text{O}_7$  at various temperatures.

In the paramagnetic state, the ZF- $\mu\text{SR}$  shows a slow muon spin relaxation caused by rapidly fluctuating dynamical

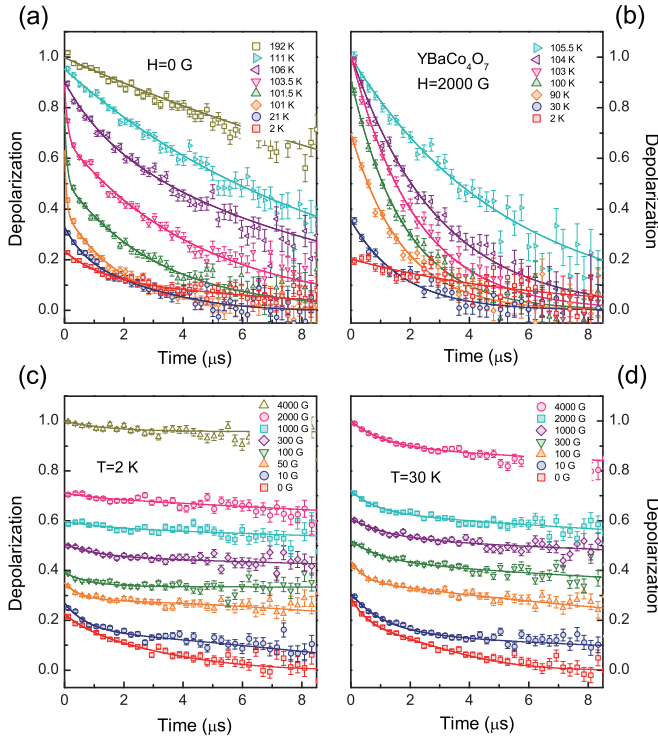


FIG. 2. (a) ZF- and (b) LF- $\mu$ SR spectra of YBaCo<sub>4</sub>O<sub>7</sub> at various temperatures. The temperature-dependent LF- $\mu$ SR spectra were recorded in a 2000 G longitudinal field to decouple the contribution of static field. LF- $\mu$ SR spectra of YBaCo<sub>4</sub>O<sub>7</sub> measured at constant temperatures (c)  $T = 2$  K and (d)  $T = 30$  K in a magnetic field  $H = 0$ –4000 G. The solid lines represent fits of the data as described in the text.

fields of Co<sup>2+</sup> and Co<sup>3+</sup> moments. As the temperature is lowered below  $T_N = 101$  K, the initial asymmetry drops rapidly without developing muon spin oscillation [see also Fig. 3(a)]. The loss of the initial asymmetry means that in the antiferromagnetically ordered state, the magnetic damping at extremely short times becomes so strong that no oscillations are detected within the electronics dead time of the continuous muon beam. At  $T = 20$  K, most of the muon spins are fully depolarized at long times and, upon further cooling to 2 K, the long-time muon polarization slightly increases, not yet reaching one-third of the initial asymmetry. It is remarkable that two distinct relaxations are clearly visible for temperatures below  $T_N$ . At short times, the fast relaxation reflects quasistatic magnetic moments while at long times, the slow relaxation is mostly dominated by dynamically fluctuating magnetic moments. It is quite unusual that a dynamical phase separation survives deep inside the magnetically ordered phase.

In an LF-decoupling experiment an external magnetic field is applied along the initial muon-spin direction. If the external field is an order of the internal static fields, the fast relaxation will be mostly quenched through a spin-locking effect. In Figs. 2(b)–2(d), the LF- $\mu$ SR spectra are shown as a function of temperature and external field. The LF- $\mu$ SR spectra recorded at constant temperatures  $T = 2$  and 30 K display a systematic shift upward with increasing field. This is consistent with the

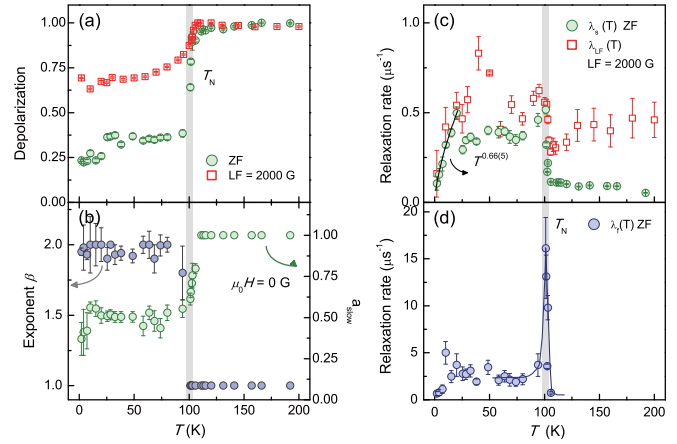


FIG. 3. (a) Temperature dependence of the initial asymmetry of YBaCo<sub>4</sub>O<sub>7</sub> extracted from the ZF- (full circles) and LF- $\mu$ SR (open squares) spectra. (b) Temperature dependence of the stretching exponent and the slow relaxing fraction of the sample obtained from the ZF data. (c) Temperature dependence of the slow muon spin-relaxation rate  $\lambda_s$  for the ZF data (full circles) and the muon relaxation rate  $\lambda_{LF}$  for the LF data (open squares). The solid curve is a fit to a power law  $\lambda_s(T) \sim T^{0.66(5)}$ . (d) Temperature dependence of the fast muon spin-relaxation rate  $\lambda_f$  taken from the ZF- $\mu$ SR spectra. The shaded bars denote the magnetic transition temperature.

formation of a static internal field below  $T_N$ . At  $T = 2$  K, a nearly full polarization of the LF- $\mu$ SR spectra occurs at  $H \approx 4$  kG, resulting in the local static field of  $\langle H \rangle_{loc} \approx 400$  G (= one tenth of 4 kG). For the  $T = 30$  K  $\mu$ SR spectra, however, there remains a significant unquenched relaxation even under the external field of 4 kG. The long-time residual slope of the LF- $\mu$ SR spectra suggests that a dynamically fluctuating field coexists with the static field, providing evidence that the kagome spins become dynamically disordered above 20 K (see below for further discussion). In addition, we applied a moderate field of 2000 G to investigate systematically spin dynamics of the dynamically fluctuating spins as a function of temperature. As seen from Fig. 2(b), the LF muon spin depolarization bears only a single component unlike the ZF data.

For a quantitative analysis, the ZF- $\mu$ SR spectra are fitted with the sum of a simple exponential function and a stretched exponential function over the full temperature range  $P_z(t) = a_{fast} \exp(-\lambda_f t) + a_{slow} \exp(-\lambda_s t)^\beta$ . Here  $\beta$  is the stretching exponent,  $\lambda_f$  ( $\lambda_s$ ) is the muon spin-relaxation rate of the fast (slow) relaxation component, and  $a_{fast}$  ( $a_{slow}$ ) is the fast (slow) relaxing fraction of the sample. For the LF- $\mu$ SR data, a single exponential function  $P_z(t) = a_{LF} \exp(-\lambda_{LF} t)$  is sufficient to describe the depolarization curves.

In Fig. 3 we summarize the temperature dependence of the obtained fit parameters for the ZF and LF data. As shown in Fig. 3(a), on cooling the depolarization of the ZF data, known to be sensitive to the onset of long-range order, exhibits a steplike drop to a roughly 1/3 value below  $T_N$  and, subsequently, shows an additional drop to 0.23 below  $T = 20$  K. The depolarization of the LF data falls gradually down to 0.68 below  $T_N$ . The volume fraction  $a_{slow}$  of the slow relaxing component levels off

to a constant value of 0.5 with decreasing temperature below  $T_N$  [see Fig. 3(b)]. At the same time, the stretch exponent increases abruptly from  $\beta = 1$  to  $\beta = 2$  below  $T_N$ . The high- $T$  exponent  $\beta = 1$  (a simple exponential function) corroborates that the relaxation rate is in the fast fluctuation limit. The exponent  $\beta = 2$  (a Gaussian relaxing function) is totally unexpected in view of the lacking recovery of the asymmetry to 1/3 in the long-range ordered state.

Noteworthy is that such a Gaussian shape of the relaxation function has been observed in the kagome system  $\text{SrCr}_8\text{Ga}_4\text{O}_{19}$ , which features a spin-liquid-like ground state [37]. The so-called undecouplable Gaussian line shape can arise when a sizable local field is sporadically present during the total muon residence time. For  $\text{SrCr}_8\text{Ga}_4\text{O}_{19}$ , a small number of unpaired spins migrating in a background of singlet spins were discussed as an origin of the Gaussian distribution of local fields. In this regard, the presence of the sporadic local fields in  $\text{YBaCo}_4\text{O}_7$  may be related to the formation of a viscous spin liquid in the kagome sublattice coexisting with the long-range ordered triangle  $\text{Co(II)}$  spins proposed by a NMR study [29].

Figures 3(c) and 3(d) show the temperature dependence of the muon spin-relaxation rates. In the high- $T$  paramagnetic phase, both  $\lambda_s(T)$  and  $\lambda_{\text{LF}}(T)$  display almost no temperature dependence, indicating that the relaxation is likely due to exchange fluctuations of the  $\text{Co}^{2+}$  and  $\text{Co}^{3+}$  spins. Using  $k_B \Theta_{\text{CW}} = 2zS(S+1)J/3$  with  $z = 4$  (6) the nearest neighbor coordination number of the  $S = 3/2$  kagome ( $S = 2$  triangular) lattice, we obtain the exchange fluctuation rate  $\nu = \sqrt{z}JS/\hbar \sim 2.0(1.3) \times 10^{13} \text{ s}^{-1}$  for the kagome (triangular) spins. Combined with the relation  $\lambda = 2\Delta^2/\nu$  in the narrowing limit,  $\lambda_s(T = 180 \text{ K}) = 0.09 \mu\text{s}^{-1}$  yields a field distribution width  $\Delta/\gamma_\mu \sim 11 \text{ kG}$ .

Upon cooling toward  $T_N$ , the fast relaxation component newly appears.  $\lambda_f(T)$  displays a  $\lambda$ -like peak, indicative of a critical slowing down of the moment fluctuations. In contrast, both  $\lambda_s(T)$  and  $\lambda_{\text{LF}}(T)$  exhibit a small kink. Overall, the spin fluctuations of the slow relaxation component slow by a factor of 2–4. The weakly growing spin-spin correlation length with temperature is characteristic of a frustrated spin system. For temperatures below 20 K, both  $\lambda_s(T)$  and  $\lambda_{\text{LF}}(T)$  show the sublinear power-law decrease  $T^{0.66(5)}$ . At a similar temperature, a crossover from the long-range ordered to the viscous spin liquid state in the kagome sublattice is deduced from NMR [29]. We further recall that the power-law behavior of the muon spin relaxation rate has been reported in other geometrically frustrated magnets [38–41]. The extracted exponent of  $\text{YBaCo}_4\text{O}_7$  is much smaller than  $n \approx 2.1$  of  $\text{Y}_2\text{Mo}_2\text{O}_7$ , which shows spin freezing at low temperatures [38,39]. As the temperature-dependent behavior of  $\lambda_s(T)$  is primarily determined by the energy dependence of magnetic excitations, the extremely weak power-law dependence suggests that the density of states of the low-energy excitations displays little dependence on energy.

$\text{YBaCo}_4\text{O}_7$  contains three crystallographically different O sites [see Fig. 1(b)]. For oxide materials, positive muons are most likely to reside near an apical  $\text{O}^{2-}$  of the oxygen tetrahedra of  $\text{Co(II)}^{2+}$  and the oxygen octahedra of  $\text{Co(I)}^{3+}$ , namely, 1 Å away from the  $\text{O}^{2-}$  ions along the  $c$  axis [40,42]. On this basis, we conclude that the fast exponentially relaxing component is mainly associated with the local dipolar

field arising from the triangle spins and the slow relaxing component is related to the kagome spins. The determined volume fraction of  $a_{\text{slow}} = 1/2$  validates this assignment. From a clear anomaly of  $\lambda_f(T)$  at  $T_N$ , we infer that the triangle spins set in the long-range magnetic order. This is contrasted by the lacking  $\lambda$ -like anomaly of  $\lambda_s(T)$ , lending support to slowly fluctuating magnetic moments in the kagome subsystem. The intermediate- $T$  dynamic magnetism in the kagome layers is due to enhanced geometrical frustration, which eventually evolves to the magnetically ordered ground state. We note that the neutron scattering and  $^{59}\text{Co}$  NMR results [26,27,29] unveil the disparate magnetism, namely the  $\text{Co(I)}^{3+}$  spins in the kagome planes remain in a dynamically disordered state down to 4 K, while the  $\text{Co(II)}^{2+}$  spins in the triangular layers order antiferromagnetically below  $T_N$ .

Next, we briefly discuss the possible origin of the initial asymmetry loss at low temperatures. As of now, the exact spin configuration of the ground state is matter of debate [28,29]. Assuming the  $120^\circ$  magnetic structure in the triangular sublattice, the crystallographically different three O sites yield the nine magnetically inequivalent muon sites. If the kagome sublattice is further taken into account, there will exist a dozen of the magnetically different muon sites. The multiple muon sites combined with magnetic inhomogeneities will lead to a broad local field distribution. This together with the large magnetic moments of  $\text{Co}^{2+}$  and  $\text{Co}^{3+}$  may explain a quick damping of the unresolved oscillating signals.

## B. $\text{YBaCo}_4\text{O}_{7.1}$

To investigate the effect of excess interstitial oxygens on magnetic behaviors, we carried out ZF- and LF- $\mu\text{SR}$  measurements of the nonstoichiometric compound  $\text{YBaCo}_4\text{O}_{7.1}$  in the temperature range of  $T = 1.55$ –200 K for two different cooling protocols. In the fast-cooling procedure, the sample was rapidly cooled at  $>10 \text{ K/min}$  from 200 to 1.55 K, while in the slow-cooling process, the sample is gradually cooled at 1 K/min. The data taken at TRIUMF and J-PARC provide the essentially same magnetism.

Figure 4 compares the temperature and cooling-rate dependencies of the ZF- $\mu\text{SR}$  spectra. At first glance, the ZF- $\mu\text{SR}$  spectra of the nonstoichiometric compound look similar to those of the stoichiometric material. For both cooling protocols, the asymmetry drops drastically upon cooling below 90 K. Similarly to the stoichiometric compound, the missing initial asymmetry is linked to the presence of a quasistatic local field originating from the large magnetic moments of  $\text{Co}^{2+}$  to  $\text{Co}^{3+}$ . This is contrasted by the  $^{59}\text{Co}$  NMR and neutron scattering results which show an unconventional spin-glass-like or a short-range ordered state with no hint for long-range magnetic order [35,36]. This discrepancy may be due to the fact that only a small fraction of the sample associated with local structural distortions gives rise to a local static field.

Neglecting the loss of the initial asymmetry, we focus on the long-time behavior of the ZF- $\mu\text{SR}$  spectra at each temperature. We find that the fast-cooling spectra are described by a simple exponential decay  $P_z(t) = a_{\text{fast}}\exp(-\lambda_f t)$  for all temperatures, while the slow-cooling spectra are fitted by the sum of a simple and stretched-exponential function:  $P_z(t) = a_{\text{fast}}\exp(-\lambda_f t) + a_{\text{slow}}\exp(-\lambda_s t)^\beta$ . Here we note that

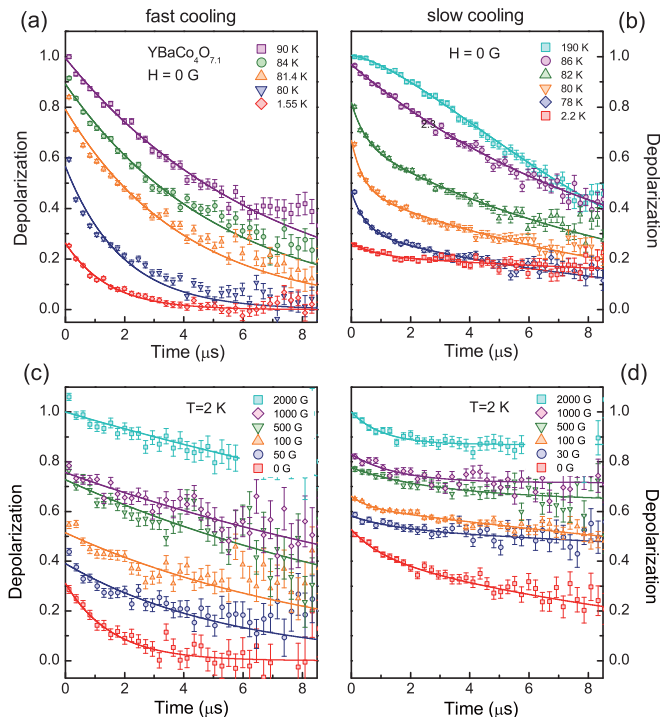


FIG. 4. Temperature dependence of the  $\mu$ SR spectra taken at TRIUMF for  $\text{YBaCo}_4\text{O}_{7.1}$  at various temperatures following (a) fast cooling ( $>10$  K/min) from 290 to 1.55 K and (b) slow cooling (1 K/min) from 290 to 2.2 K. LF- $\mu$ SR spectra of  $\text{YBaCo}_4\text{O}_{7.1}$  measured at  $T = 2$  K on (c) fast cooling and (d) slow cooling in a magnetic field  $H = 0$ –2000 G. The solid lines represent fits of the data as described in the text.

a line shape of the ZF- $\mu$ SR spectra relies on the cooling rate of the sample.

In Fig. 5 we summarize the temperature dependence of the extracted parameters. The depolarization of the ZF data shows a steplike drop to a value of about 0.3 with decreasing temperature through 90 K. This together with the absence of a recovery of the asymmetry to 1/3 points towards the occurrence of a partial static field. For the fast-cooling protocol, the muon spin relaxation is governed by a rapidly fluctuating dynamical field with a single relaxation rate at all temperatures. At high temperatures above 90 K, the muon spins are weakly relaxing. Upon cooling towards 90 K, the muon spin relaxation exhibits a steep increase and levels off, indicating a slowing down of the moment fluctuations and a subsequent persistence of slow spin dynamics. The persistent spin dynamics has been reported in a range of frustrated magnets whose ground states are spin liquid, spin freezing, and a weak magnetic order [43]. At the moment, there is no unified explanation on the underlying mechanism, yet it is largely understood in terms of unconventional low-energy excitations.

Here we recall that the excess oxygens are located either under the kagome planes or at the face center of the Ba anticuboctahedra [44]. The small structural disorders induced by the incorporation of the extra oxygen atoms convert a fraction of oxygen tetrahedra surrounding Co ions into octahedra [34]. The major impact of the structural disorders is to prevent the structural transition, while retaining the crystal

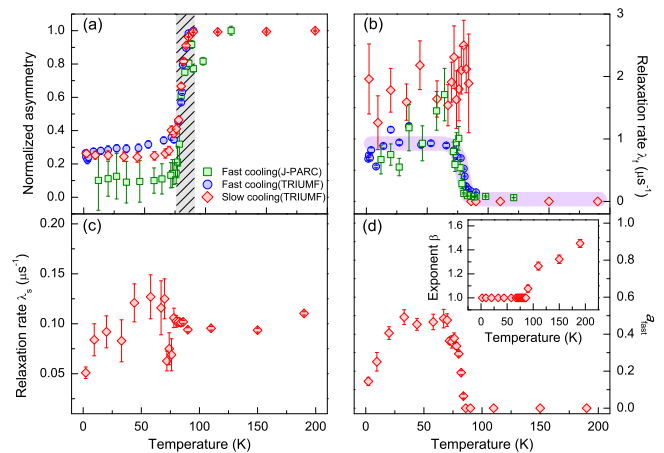


FIG. 5. (a) Temperature dependence of the normalized initial asymmetry of  $\text{YBaCo}_4\text{O}_{7.1}$  extracted from the  $\mu$ SR spectra. (b) Muon relaxation rate  $\lambda_f$  and (c)  $\lambda_s$  of  $\text{YBaCo}_4\text{O}_{7.1}$  as a function of temperature, obtained from the  $\mu$ SR spectra. (d) Temperature dependence of the fast relaxing fraction of the sample. The inset shows the change of the exponent with temperature.

symmetry  $P31c$  down to 6 K [36]. The preservation of the original high-symmetry lattice eliminates a route to relieve the geometrical frustration, being in favor of short-range magnetic fluctuations. In course of the fast-cooling process, the randomly distributed excess oxygen atoms are quenched without forming the inhomogeneous oxygen clusters. As a result, there will be multiple muon sites, leading to multiple fluctuation rates and/or wide field distribution widths. According to a  $^{59}\text{Co}$  zero-field NMR study [35], the kagome spins fluctuate much faster than the triangular spins. Nevertheless, the observed single relaxation rate means that the magnetic fluctuations of the kagome and triangle spins are effectively indistinguishable in the time window of the muon decay. Taken together,  $\text{YBaCo}_4\text{O}_{7.1}$  does not exhibit the long-range magnetic order on either sublattice. Thus, the local static field may be caused by the local structural distortions created by the interstitial oxygens, which promote the magnetic symmetry breaking through magnetoelastic coupling.

We now turn to the slow-cooling results. Unlike the fast-cooling procedure, the slow-cooling ZF- $\mu$ SR spectra contain the fast relaxing component below 90 K as in the case of the stoichiometric compound. However, their relaxation line shape is not the same. As the temperature is lowered to 90 K, the exponent decreases from a value of  $\beta = 1.5$  to  $\beta = 1$  [see the inset of Fig. 5(d)]. In addition, as shown in Figs. 5(b) and 5(c), the fast muon relaxation rate  $\lambda_f(T)$  displays a plateau below 70 K; a clear indicator of persistent spin dynamics. It should be noted that the relaxation rate  $\lambda_f(T) \sim 2 \mu\text{s}^{-1}$  for the slow-cooling measurements is larger than that for the fast-cooling experiments. The slow relaxing fraction  $a_{\text{slow}}$  increases to a value of 0.5 on cooling toward 70 K and then decreases gradually below 30 K. The slow relaxation rate  $\lambda_s(T)$  shows little dependence on temperatures down to 50 K and tends to decrease slightly below 50 K. The small value of  $\lambda_s(T) \sim 0.1 \mu\text{s}^{-1}$  implies the presence of fast electron spin fluctuations in some regions of the crystal, which persist down to low temperatures.

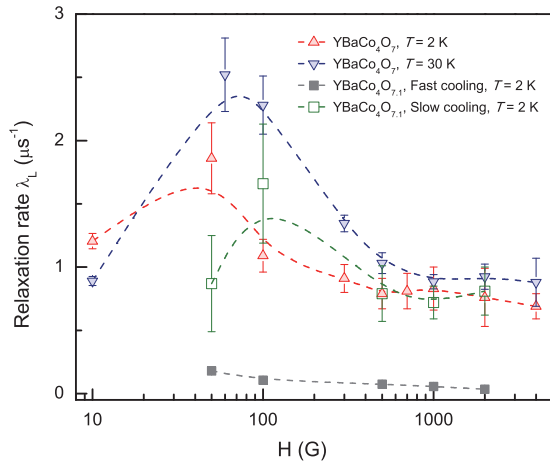


FIG. 6. Field dependence of the longitudinal relaxation rate of  $\text{YBaCo}_4\text{O}_7$  measured at  $T = 2$  K (full triangles) and 30 K (inverse full triangles) and  $\text{YBaCo}_4\text{O}_{7.1}$  recorded at  $T = 2$  K in the fast (full squares) and slow (open squares) cooling processes. An external field is plotted in a logarithmic scale.

The bifurcation of the two different relaxing components at 90 K suggests the existence of two distinct magnetic entities at low temperatures. Indeed, the slow-cooling NMR measurements of  $\text{YBaCo}_4\text{O}_{7.1}$  showed that the interstitial inhomogeneous oxygen clustering occurs into oxygen-rich regions and oxygen-poor regions [35]. The oxygen-poor regions resemble the stoichiometric material while the oxygen-rich regions are characteristic of a paramagnetic state. In spite of the obvious inhomogeneous magnetism, it is striking that the stretch parameter is not smaller than  $\beta = 1$ . Here we stress that the two simple exponential relaxation rates below 90 K preclude a broad distribution of electron spin correlation times at least in the  $\mu\text{SR}$  frequency domain as well as the formation of conventional spin-glass-like state, in which the exponent approaches  $\beta = 1/3$  [45,46]. Rather, the muon spins probe the local static field coexisting with fluctuating internal magnetic fields having the two unique correlation times, which differ by an order of magnitude. This is in stark contrast to the low  $\beta = 0.3\text{--}0.45$  values observed in the stretched exponential recovery of the nuclear magnetization [35]. At the moment, the origin of the apparent contradiction between the NMR and the  $\mu\text{SR}$  data is far from clear. Possibly, the muon spin relaxation is substantially influenced by the phase separation process involving the oxygen migration. In addition, the locally symmetry-reduced regions generated by the structural inhomogeneities can bring about the local static field, resulting in the missing initial asymmetry.

Figure 6 presents the longitudinal relaxation rate  $\lambda_L$  as a function of an external field.  $\lambda_L(H)$  shows a narrow peak at about 70 G, reflecting the competition between the static and dynamic components of the local field at the muon site. The occurrence of such a peak means a broad distribution of spin-spin correlation times. For applied fields above 100 G, the field dependence of  $\lambda_L(H)$  is largely determined by the long-lived local field fluctuations. Noticeably,  $\lambda_L(H)$  for the fast-cooled  $\text{YBaCo}_4\text{O}_{7.1}$  compound is an order of magnitude smaller than that for both the pristine  $\text{YBaCo}_4\text{O}_7$  and the

slow-cooled  $\text{YBaCo}_4\text{O}_{7.1}$  compound. Accordingly, the triangle and kagome spins behave more dynamically in the fast-cooled  $\text{YBaCo}_4\text{O}_{7.1}$  than in both the pristine and the slow-cooled  $\text{YBaCo}_4\text{O}_{7.1}$  compound.

#### IV. CONCLUSION

The geometrically frustrated antiferromagnets  $\text{YBaCo}_4\text{O}_{7+\delta}$  ( $\delta = 0, 0.1$ ) have been investigated by ZF- and LF- $\mu\text{SR}$  measurements. Our results of the stoichiometric compound uncover a disparate development of magnetic order between the two kagome and triangle sublattices. The loss of asymmetry and  $\lambda$ -like behavior of the fast relaxation component indicate that the triangular spins first order at  $T_N = 101$  K. In contrast to the establishment of static magnetism in the triangular layers, the dynamic magnetism in the kagome layer is evident from the ZF- and LF- $\mu\text{SR}$  data that feature persistent spin dynamics in the intermediate temperatures between 20 K and  $T_N$ . Subsequently, upon cooling towards  $T = 4$  K, the sublinear decrease of the slow relaxation rate confirms a transition to long-range order with unconventional low-energy excitations.

On introducing a small amount of interstitial oxygen atoms, we find the drastically different magnetic behavior of the nonstoichiometric compound. This is mainly because the preservation of the trigonal lattice symmetry disallows relieving geometrical frustration, thereby leading to the more dynamic spin fluctuations in the nonstoichiometric than in the stoichiometric material. Similarly to the stoichiometric compound, the drop of asymmetry below 90 K indicates the formation of quasistatic internal fields. In spite of the weak static field, the long-time muon relaxation rate exhibits the persistence of dynamic magnetism to low temperatures, irrespective of a cooling rate. The fast-cooled  $\mu\text{SR}$  spectra show a simple exponential line shape, implying that most of spins fluctuate dynamically within a single spin correlation time in the muon time window. The slow-cooled spectra below 90 K are described with a sum of a simple exponential and stretched exponential function. The stretch exponent approaches a value of  $\beta = 1$  upon cooling towards 90 K. The bifurcation of the  $\mu\text{SR}$  spectra into the fast and slow relaxing components with two largely different time scales of electron spins is consistent with a phase separation into interstitial oxygen-poor and oxygen-rich regions in the slow-cooling process. Despite the obvious local magnetic inhomogeneity, the muon spins do not probe a broad distribution of internal fields. This is discussed in terms of a sporadic distribution of local fields, conspired by oxygen migration and a  $120^\circ$  spin structure of the triangular sublattice.

In the frustrated system comprising interpenetrating kagome and triangle sublattices, dynamic and static magnetism is intriguingly intertwined in a single material and its spin-spin correlation times can be tuned by varying parameters such as structural symmetry and inhomogeneity.

#### ACKNOWLEDGMENTS

This work was supported by the Korea Research Foundation (KRF) grant funded by the Korea government (MEST) (Grants No. 2009-0093817, No. 20170211, and No. 20170675).

- [1] L. Balents, *Nature (London)* **464**, 199 (2010).
- [2] R. Moessner and J. T. Chalker, *Phys. Rev. B* **58**, 12049 (1998).
- [3] O. Tchernyshyov, R. Moessner, and S. L. Sondhi, *Phys. Rev. Lett.* **88**, 067203 (2002).
- [4] R. R. P. Singh and D. A. Huse, *Phys. Rev. Lett.* **68**, 1766 (1992).
- [5] P. Sindzingre, P. Lecheminant, and C. Lhuillier, *Phys. Rev. B* **50**, 3108 (1994).
- [6] L. Capriotti, A. E. Trumper, and S. Sorella, *Phys. Rev. Lett.* **82**, 3899 (1999).
- [7] Z. Weihong, R. H. McKenzie, and Rajiv R. P. Singh, *Phys. Rev. B* **59**, 14367 (1999).
- [8] H. Morita, S. Watanabe, and M. Imada, *J. Phys. Soc. Jpn.* **71**, 2109 (2002).
- [9] S. Yunoki and S. Sorella, *Phys. Rev. B* **74**, 014408 (2006).
- [10] O. I. Motrunich, *Phys. Rev. B* **72**, 045105 (2005).
- [11] W.-J. Lee, S.-H. Do, S. Yoon, S. Lee, Y. S. Choi, D. J. Jang, M. Brando, M. Lee, E. S. Choi, S. Ji, Z. H. Jang, B. J. Suh, and K.-Y. Choi, *Phys. Rev. B* **96**, 014432 (2017).
- [12] Y. Ran, M. Hermele, P. A. Lee, and X.-G. Wen, *Phys. Rev. Lett.* **98**, 117205 (2007).
- [13] H. C. Jiang, Z. Y. Weng, and D. N. Sheng, *Phys. Rev. Lett.* **101**, 117203 (2008).
- [14] S. Yan, D. Huse, and S. White, *Science* **332**, 1173 (2011).
- [15] H. C. Jiang, Z. Wang, and L. Balents, *Nat. Phys.* **8**, 902 (2012).
- [16] S. Depenbrock, I. P. McCulloch, and U. Schollwöck, *Phys. Rev. Lett.* **109**, 067201 (2012).
- [17] S.-S. Gong, W. Zhu, L. Balents, and D. N. Sheng, *Phys. Rev. B* **91**, 075112 (2015).
- [18] H. J. Liao, Z. Y. Xie, J. Chen, Z. Y. Liu, H. D. Xie, R. Z. Huang, B. Normand, and T. Xiang, *Phys. Rev. Lett.* **118**, 137202 (2017).
- [19] T.-H. Han *et al.*, *Nature (London)* **492**, 406 (2012).
- [20] M. Valldor and M. Andersson, *Solid State Sci.* **4**, 923 (2002).
- [21] M. Valldor, *Solid State Sci.* **6**, 251 (2004).
- [22] D. D. Khalyavin, P. Manuel, J. F. Mitchell, and L. C. Chapon, *Phys. Rev. B* **82**, 094401 (2010).
- [23] S. Buhandt and L. Fritz, *Phys. Rev. B* **90**, 020403(R) (2014).
- [24] A. Huq, J. F. Mitchell, H. Zheng, L. C. Chapon, P. G. Radaelli, K. S. Knight, and P. W. Stephens, *J. Solid State Chem.* **179**, 1136 (2006).
- [25] N. Hollmann, Z. Hu, M. Valldor, A. Maignan, A. Tanaka, H. H. Hsieh, H.-J. Lin, C. T. Chen, and L. H. Tjeng, *Phys. Rev. B* **80**, 085111 (2009).
- [26] L. C. Chapon, P. G. Radaelli, H. Zheng, and J. F. Mitchell, *Phys. Rev. B* **74**, 172401 (2006).
- [27] D. D. Khalyavin, P. Manuel, B. Ouladdiaf, A. Huq, P. W. Stephens, H. Zheng, J. F. Mitchell, and L. C. Chapon, *Phys. Rev. B* **83**, 094412 (2011); **83**, 219902(E) (2011).
- [28] P. Manuel, L. C. Chapon, P. G. Radaelli, H. Zheng, and J. F. Mitchell, *Phys. Rev. Lett.* **103**, 037202 (2009).
- [29] M. J. R. Hoch, P. L. Kuhns, S. Yuan, T. Besara, J. B. Whalen, T. Siegrist, A. P. Reyes, J. S. Brooks, H. Zheng, and J. F. Mitchell, *Phys. Rev. B* **87**, 064419 (2013).
- [30] M. Karppinen, H. Yamauchi, S. Otani, T. Fujita, T. Motohashi, Y.-H. Huang, M. Valkeapää, and H. Fjellvåg, *Chem. Mater.* **18**, 490 (2006).
- [31] S. Räsänen, H. Yamauchi, and M. Karppinen, *Chem. Lett.* **37**, 638 (2008).
- [32] H. Hao, L. Zhao, J. Hu, X. Hu, and H. Hou, *J. Rare Earths* **27**, 815 (2009).
- [33] Y. Jia, H. Jiang, M. Valkeapää, H. Yamauchi, M. Karppinen, and E. I. Kauppinen, *J. Am. Chem. Soc.* **131**, 4880 (2009).
- [34] O. Chmaissem, H. Zheng, A. Huq, P. W. Stephens, and J. F. Mitchell, *J. Solid State Chem.* **181**, 664 (2008).
- [35] S. Yuan, X. Hu, P. L. Kuhns, A. P. Reyes, J. S. Brooks, T. Besara, T. Siegrist, H. Zheng, J. F. Mitchell, and M. J. R. Hoch, *Phys. Rev. B* **89**, 094416 (2014).
- [36] S. Avci, O. Chmaissem, H. Zheng, A. Huq, P. Manuel, and J. F. Mitchell, *Chem. Mater.* **25**, 4188 (2013).
- [37] Y. J. Uemura, A. Keren, K. Kojima, L. P. Le, G. M. Luke, W. D. Wu, Y. Ajiro, T. Asano, Y. Kuriyama, M. Mekata, H. Kikuchi, and K. Kakurai, *Phys. Rev. Lett.* **73**, 3306 (1994).
- [38] S. R. Dunsiger, R. F. Kiefl, K. H. Chow, B. D. Gaulin, M. J. P. Gingras, J. E. Greedan, A. Keren, K. Kojima, G. M. Luke, W. A. MacFarlane, N. P. Raju, J. E. Sonier, Y. J. Uemura, and W. D. Wu, *Phys. Rev. B* **54**, 9019 (1996).
- [39] S. R. Dunsiger, R. F. Kiefl, K. H. Chow, B. D. Gaulin, M. J. P. Gingras, J. E. Greedan, A. Keren, K. Kojima, G. M. Luke, W. A. MacFarlane, N. P. Raju, J. E. Sonier, Y. J. Uemura, and W. D. Wu, *J. Appl. Phys.* **79**, 6636 (1996).
- [40] S. R. Dunsiger, A. A. Aczel, C. Arguello, H. Dabkowska, A. Dabkowski, M.-H. Du, T. Goko, B. Javanparast, T. Lin, F. L. Ning, H. M. L. Noad, D. J. Singh, T. J. Williams, Y. J. Uemura, M. J. P. Gingras, and G. M. Luke, *Phys. Rev. Lett.* **107**, 207207 (2011).
- [41] S. T. Bramwell, S. R. Giblin, S. Calder, R. Aldus, D. Prabhakaran, and T. Fennell, *Nature (London)* **461**, 956 (2009).
- [42] E. Holzschuh, A. B. Denison, W. Kundig, P. F. Meier, and B. D. Patterson, *Phys. Rev. B* **27**, 5294 (1983).
- [43] A. Yaouanc, P. Dalmas de Reotier, A. Bertin, C. Marin, E. Lhotel, A. Amato, and C. Baines, *Phys. Rev. B* **91**, 104427 (2015).
- [44] M. Valldor, in *New Topics in Condensed Matter Research*, edited by J. V. Chang (Nova Science, New York, 2007), pp. 75–102.
- [45] I. A. Campbell, A. Amato, F. N. Gygax, D. Herlach, A. Schenck, R. Cywinski, and S. H. Kilcoyne, *Phys. Rev. Lett.* **72**, 1291 (1994).
- [46] A. Keren, P. Mendels, I. A. Campbell, and J. Lord, *Phys. Rev. Lett.* **77**, 1386 (1996).